Geoderma 368 (2020) 114308

Contents lists available at ScienceDirect

Geoderma

journal homepage: www.elsevier.com/locate/geoderma

Neoformed aluminosilicate and phytogenic silica are competitive sinks in the silicon soil–plant cycle

Zimin Li[a,*], Jean-Thomas Cornelis[b], Charles Vander Linden[a], Eric Van Ranst[c], Bruno Delvaux[a]

[a] Université catholique de Louvain (UCLouvain), Earth and Life Institute, Soil Science, Louvain-La-Neuve 1348, Belgium
[b] University of Liège, Gembloux Agro-Bio Tech, TERRA Teaching and Research Centre, 5030 Gembloux, Belgium
[c] Ghent University, Department of Geology (WE13), Gent, Belgium

ARTICLE INFO

Handling Editor: David Laird

Keywords:
Phytolith
Allophane
Rice
Weathering
Silicon cycle
Biochar

ABSTRACT

In soils, mineral weathering and phytolith dissolution release aqueous monosilicic acid that can be taken up by plant, adsorbed on mineral surfaces, entrapped in neoformed clay minerals, or exported to watersheds. The balance between biotic and abiotic processes determines the fluxes of bioavailable silicon (Si), impacting plant growth and health, and diatoms biomass, hence the oceanic capacity to fix carbon dioxide. Here we quantified this balance in an experimental system using rice and an albic soil material (quartz grains) containing no weatherable silicate minerals. Materials representing a soil weathering gradient were prepared by adding variable amounts of silicate minerals within fresh powdered tephrite (< 83 μm) as a source of weatherable minerals whereas phytogenic Si was supplied within phytolith-rich biochar. We quantified the distribution of Si in leachate, soil and plant reservoirs. Weatherable minerals rapidly released Si that flowed into two main sinks: allophanic substances neoformed in soil from released Si and aluminum (Al), and phytoliths formed by precipitation of absorbed silica in plant tissues. The leaching of Si was negligible. Allophane rapidly formed at a maximum rate of 0.85 g allophane kg^{-1} soil day^{-1}. Of the Si stock of weatherable minerals, 7–14% contributed to allophanic Si and less than 1% to phytogenic Si. The contribution of supplied phytoliths to plant Si accumulation markedly increased from 26 to 80% with the decrease in weatherable mineral reserve from 405 to 5 $cmol_c$ kg^{-1}. Weatherable minerals primarily controlled bioavailable Si while phytoliths increasingly contributed to Si plant uptake with increasing mineral depletion. Returning phytoliths to soil thus boosts the biological recycling of Si in proportion to the increase in soil weathering stage.

1. Introduction

The continental cycle of silicon (Si) is mainly based on the Si soil–plant cycle where the primary source of Si is the reserve of weatherable lithogenic aluminosilicates (McKeague and Cline, 1963a; Alexandre et al., 1997; Sommer et al., 2006; Henriet et al., 2008b). In soils, the dissolution of lithogenic aluminosilicates releases aqueous $H_4SiO_4^0$ (dissolved Si: DSi), aluminum (Al), iron (Fe) and other solutes. Some of these may recombine to form pedogenic minerals such as secondary aluminosilicates, Al and Fe oxides. Pedogenic aluminosilicates can in turn dissolve depending on the activity of DSi (Garrels and Christ, 1965; Kittrick, 1977; Lindsay, 1979). At advanced soil Si depletion stage, Al and Fe oxides accumulate and may enhance adsorption of $H_4SiO_4^0$ (Beckwith and Reeve, 1963; Jones and Handreck, 1963; McKeague and Cline, 1963b; Struyf et al., 2009; Churchman and Lowe, 2012; Song et al., 2012). The processes of lithogenic aluminosilicates weathering, pedogenic aluminosilicate neoformation and dissolution, and DSi adsorption define the mineral contribution of lithogenic and pedogenic aluminosilicates to the DSi pool. These contributions govern the mobility of Si in moderately weathered soils where both types of aluminosilicates act as major sources and sinks of Si (Cornelis and Delvaux, 2016). Yet DSi can be taken up by plant roots, translocated to plant shoots (Jones and Handreck, 1965), and precipitate as amorphous Si, called phytoliths (PhSi), which return to soil within plant residues (Smithson, 1956; Farmer et al., 2005). PhSi particles readily dissolve (Köhler et al., 2005; Fraysse et al., 2006, 2009), and replenish the DSi pool in soil. The processes of DSi uptake, PhSi formation and dissolution define the biological Si feedback loop, which governs the mobility of Si in highly weathered soils. Recent meta-analyses suggest that the biological Si feedback loop may progressively take over the mineral cycle along a soil weathering gradient (Cornelis and Delvaux, 2016; Vander Linden and Delvaux, 2019). Thus, paradoxically, the contribution of

* Corresponding author at: Earth and Life Institute, Soil Sciences, Université catholique de Louvain, Croix du Sud 2/L7.05.10, 1348 Louvain-la-Neuve, Belgium.
E-mail address: zimin.li@uclouvain.be (Z. Li).

https://doi.org/10.1016/j.geoderma.2020.114308
Received 8 January 2020; Received in revised form 25 February 2020; Accepted 29 February 2020

PhSi to Si biocycling would be more important in soils depleted in lithogenic and pedogenic aluminosilicates, and depends on the biological pumping of Si (Lucas et al., 1993; Meunier et al., 1999; Lucas, 2001; Carey and Fulweiler, 2012; Vander Linden and Delvaux, 2019). However, the respective contributions of lithogenic silicates and phytoliths to Si biocycling has not yet been addressed and quantified in controlled experiments despite its importance in croplands on highly weathered soils.

In agrosystems, crop harvesting disrupts the biological Si feedback loop (Meunier et al., 2008; Guntzer et al., 2012; Keller et al., 2012; Haynes, 2017). In the long term, PhSi and DSi pools may decrease (Struyf et al., 2010; Vandevenne et al., 2012) whereas detrimental effects on crop yield may occur. Indeed, Si exerts major positive effects on plants by increasing their photosynthetic activity and tolerance against various biotic and abiotic stresses (Epstein, 1994; Belanger, 1995; Exley, 1998; Fauteux et al., 2005; Liang et al., 2007). Both the natural soil Si depletion and removal of crop residues from Si high-accumulator plants thus contribute to Si depletion in soils (Vander Linden and Delvaux, 2019). Therefore, the enhancement of the biological Si feedback loop presents a major agronomic interest, particularly in croplands on highly weathered soils (Li and Delvaux, 2019).

The supply of pyrolyzed biomass is known to improve soil fertility through the increase of pH, organic carbon (OC) content, and cation exchange capacity (CEC), promoting plant growth (Liang et al., 2006; Major et al., 2010; Sohi et al., 2010; Jeffery et al., 2011; Crane-Droesch et al., 2013; Lehmann and Joseph, 2015). Such a supply may enhance the biological Si feedback loop. Indeed, plant-derived phytoliths are concentrated in biochar (Xiao et al., 2014; Li and Delvaux, 2019). Their increased solubility, which is enhanced after burning (Ngoc Nguyen et al., 2014; Unzué-Belmonte et al., 2016; Li and Delvaux, 2019), enhances their ability to release plant-available Si (Houben et al., 2014; Liu et al., 2014; Wang et al., 2018a; Wang et al., 2018b), which can be taken up by plant roots (Li et al., 2018; Li et al., 2019). The amplitude of plant Si uptake and mineralomass depends, however, on plant species, soil weathering stage, pH and buffer capacity (Li et al., 2019).

Here we use dosed additions of lithogenic aluminosilicates and PhSi-biochar input to boost, respectively, the mineral contribution and the biological Si feedback loop in the Si soil–plant cycle. We investigate the Si dynamics in a soil–plant system using rice plant and controlling lithogenic aluminosilicate and PhSi inputs in order to quantify the balance between the mineral contribution and biological Si feedback loop, which is unknown.

2. Materials and methods

2.1. Soil materials

The initial soil used was albic material (E horizon) of a Podzol (*Spodosol*) developed on sandy sediments of the Brussels Formation (Eocene), located in the *Bois de Lauzelle*, Louvain-la-Neuve, central Belgium. The altitude is ~90 m.a.s.L.; the climate is humid temperate with mean annual temperature and precipitation of 9.4 °C and 835 mm, respectively. The albic horizon was 35 cm thick. A sample was air-dried and sieved at 2 mm prior to further characterization. Quartz was the exclusive mineral, as evidenced by X-ray diffraction (XRD) (Fig. S1a, Supplementary data) and SiO_2 content was in accord with this composition (98.63%, Table S1). Table S1 further shows that amorphous silica and bioavailable Si contents were negligible as inferred from, respectively, oxalate- and Na_2CO_3- extractable Si (0 and < 0.02 g kg^{-1}), and $CaCl_2$ extractable Si (0.03 g kg^{-1}) contents. The organic carbon content (0.3 g kg^{-1}) was negligible. The total reserve in bases (TRB), which sums the total contents of major alkaline and alkaline-earth cations to estimate the reserve of weatherable primary minerals (Herbillon, 1986), amounted to 5 $cmol_c$ kg^{-1} (Table S1), a content much below 40 $cmol_c$ kg^{-1}, considered as the upper limit for highly weathered ferrallitic soils (Herbillon, 1986).

We used fresh tephrite as a source of weatherable lithogenic aluminosilicates. This material was obtained from DCM Inc.Co. www.dcm-info.com as a powder (< 83 μm) of fresh natural tephritic lava (Eifel, Germany) crushed and sieved at 83 μm. It was rich in weatherable lithogenic aluminosilicates as it contained augite, olivine, leucite, nepheline, plagioclase and phlogopite (Fig. S1. b), but no (or minor) glass. The TRB amounted to 1058 $cmol_c$ kg^{-1} (Table S1). The respective cation contents ($cmol_c$ kg^{-1}) decreased in the order Mg (447) > Ca (4 2 8), > Na (97) > K (85), representing, respectively, 42, 40, 9 and 8% of TRB. Dosed quantities of fresh tephrite were added to the albic soil material to simulate a soil weathering gradient following a TRB geometric progression using three as a constant multiplying factor, i.e. from TRB ($cmol_c$ kg^{-1}) 5 to 15, 45, 135 and 405 $cmol_c$ kg^{-1}. Tephrite:Podzol-E mixtures were built up by respective tephrite additions of 0, 10, 38, 123 and 308 g kg^{-1} soil (dry weight) to reach the respective TRB values. The two components were mixed thoroughly and homogeneously using a plastic bag to reach 2 kg on a dry weight basis. The mixtures Tephrite:Podzol-E were thus considered as synthetic soils named here soils T5, T15, T45, T135 and T405, respectively (T for TRB). Here, these soils will be used (i) uncultivated; (ii) cultivated using rice crop without biochar supply; cultivated with rice crop but previously amended with (iii) phytolith-free biochar (Si−) or (iv) phytolith-rich biochar (Si+). The simulated weathering gradient from TRB 405 to 5 $cmol_c$ kg^{-1} is perfect in line with weathering sequences starting from young Cambisols or Andosols to highly weathered soils (Delvaux et al., 1989; Henriet et al., 2008a; Klotzbücher et al., 2015; Vermeire et al., 2016).

2.2. Biochar materials

The Si depleted and Si enriched biochars (Si− and Si+) were produced from rice straws (RS). Rice seeds (*Oryza sativa* subsp. indica IR64 from IRRI, Philippines) germinated on a polystyrene plate floating on a Yoshida nutrient solution (Yoshida, 1981) in 10 plastic tanks each of 25 L. Si− and Si+ rice plants were each produced in five respective tanks. After one week, the solutions for Si+ plants were enriched with aqueous $H_4SiO_4^0$ at a concentration of 40 mg L^{-1}. $H_4SiO_4^0$ was prepared through dissolving $Na_2SiO_3{\cdot}5H_2O$, and further leaching on an H^+ cation exchanger (Amberlite®IR-120) to fix Na^+ ions until the threshold level of Na^+ was below 10^{-2} mM Na (Henriet et al., 2006). Si− and Si+ nutrient solutions were renewed weekly. After two weeks, the seedlings were thinned to one plant per hole. The pH was adjusted daily to 5.0–5.3 by using 2 M KOH or HCl. Si− and Si+ plants were grown in greenhouse-controlled conditions: 80% relative humidity, 28/25 °C day/night, 12 h photoperiod with 360 μmol m^{-2} s^{-1} light intensity. After 12 weeks, the plants were harvested. The aboveground biomass was measured fresh, then dry after 7 days at 55 °C. The biochars were obtained from Si− and Si + rice straws, respectively, according to a slow pyrolysis procedure (Ronsse et al., 2013). Dried straws (2 cm fragments) were placed in a vertical, tubular, stainless steel reactor (d × L = 3.8 × 30 cm), and further pyrolyzed at a heating rate of 17 °C min^{-1} up to 500 °C. The reactor was maintained at 500 °C for 60 min, and then progressively cooled. Nitrogen was continuously supplied to remove gases and tars produced during the pyrolysis process. Biochar yields were calculated as the mass ratio of biochar to the dried RS used for the pyrolysis process. The Si-enriched (Si+) and Si-depleted (Si−) biochars were passed through a 0.154 mm sieve prior to experimental use.

2.3. Soil:biochar mixtures

The soil:biochar mixtures were prepared by adding Si− and Si+ biochar to the soil at the rate of 2.5 g biochar per kg of soil resulting in supplying 3 mg PhSi per kg to the five Si-soil mixtures (Si-T5, Si-T15, Si-T45, Si-T135, Si-T405), and 121 mg PhSi per kg to the five Si+soils mixtures (Si+T5, Si+T15, Si+T45, Si+T135, Si+T405). This rate is

equivalent to supply 2.8 T biochar ha^{-1}, and, in the case of Si+, 136.5 kg Si ha^{-1}, which correspond to field application rates of, biochar (Liu et al., 2013) and Si fertilizers (Savant et al., 1996; Ma and Takahashi, 2002), respectively.

2.4. Soil-plant experimental device

The experimental device is sketched out in Fig. S2 (Supplementary data). Two kg of soil or soil:biochar mixture was packed into each pot. Four treatments were designed, each with five replicates: (a) bare soils, (b) rice-cropped soils without biochar, (c) rice cropped soils with Si-biochar, and (d) rice cropped soils with Si + biochar. They were respectively named: (a) bare soils T5, T15, T45, T135, T405, (b) rice cropped soils T5, T15, T45, T135, T405, (c) Si-biochar amended cropped soils Si-T5, Si-T15, Si-T45, Si-T135, Si-T405, and (d) Si + biochar amended-cropped soils Si + T5, Si + T15, Si + T45, Si + T135, Si + T405. Two successive rice cropping periods each of 13 weeks were conducted in controlled phytotron conditions: 80% relative humidity, day/night temperature 30/25 °C, 12 h photoperiod with 360 μmol m^{-2} s^{-1} light intensity.

2.4.1. 1st cropping period

Soils and soil:biochar mixtures were irrigated with deionized water and kept for a four-week incubation at field moisture capacity during 4 weeks before rice cropping. After germination in deionized water, the rice plantlets (*Oryza sativa* subsp.*indica*, IR64) were allowed to grow up to 5 cm height. Three plantlets were transplanted in each pot. During rice growth, each pot was watered every two days with 100 mL deionized water during the first 4 weeks, and 200 mL the last 9 weeks. Nitrogen fertilizer (15 mg kg^{-1}, 17 kg N ha^{-1}) was applied as NH_4NO_3 to all treatments, and split into three applications: 20% at week 2, 40% at week 4, and 40% at week 6. At week 13, the aboveground plant part was collected to separate straws and grains for washing with deionized water, and drying at 55 °C for 7 days before weighing their dry matter (DM). The dried rice straws were considered as crop residues and crashed (< 2 cm) for restitution to soil:biochar mixtures prior the 2nd cropping period.

2.4.2. 2nd cropping period

The respective rice straws (RS) (3 g pot^{-1}) collected from the 1st cropping period were returned to their respective soil:biochar mixtures. Rice straws were not returned to bare soils and soils were cultivated without a biochar supply to simulate distinct cropping practices that either minimize or maximize crop residues and use of biochar. After rice crop harvesting from the first cropping, all soils and soil:biochar mixtures were watered once a week with 200 mL deionized water and kept for a 4-week incubation at field moisture capacity before the 2nd rice cropping, which was carried out following the same protocol applied for the first cropping period.

2.5. Chemical analyses

2.5.1. Soils and soil:biochar mixtures

Total elemental contents of Si, Al, Fe, Ca, K, Na and Mg were determined prior to the 1st cropping by inductively coupled plasma/atomic emission spectrometry (ICP–AES, Jarrell Ash Iris Advantage) after alkaline fusion using Li-metaborate + Li-tetraborate at 1000 °C, followed by ash dissolution with concentrated HNO_3 (Chao and Sanzolone, 1992). The pH in H_2O and 1 M KCl were measured using 5 g:25 mL suspensions. The C and N contents (and H for RS and biochars) were measured using a Flash 2000 Elemental Analyzer (Thermo Fisher Scientific, Waltham, MA, USA). The CEC and contents of exchangeable cations were determined using 1 M CH_3COONH_4 buffered at pH = 7 (Chapman, 1965). Crystalline soil minerals were identified by X-ray diffraction (XRD) on soil powder samples using CuKα radiation in a Bruker Advance diffractometer. Soil textural analysis was achieved by quantitative recovery of clay, silt and sand fractions after sonication and dispersion with Na^+-saturated resins without any previous H_2O_2 oxidation of organic matter (Bartoli et al., 1991). Scanning electron microscopy coupled with energy dispersive X-ray analysis (SEM-EDX) was performed on biochar without any chemical pretreatment using a field emission gun SEM (FEG-SEM; Zeiss Ultra55) equipped with an EDX system (Jeol JSM2300 with a resolution < 129 eV), and operating at 15 keV with a working distance of 8 mm. The acquisition time of the EDX spectra lasted 100 s with a probe current of 1 nA.

2.5.2. Rice plant materials and biochars

Harvested straws and grains were dried at 55 °C for 7 days prior to weigh their dry matter (DM). The dried plant materials were analyzed for selected elements (C, N, H, Si, K, Ca, Na and Mg). Total carbon (C), nitrogen (N), and hydrogen (H) contents were measured by dry combustion with a CNHS analyzer (Flash EA1112 Series). Oxygen (O) was computed as follows: oxygen (O) (%) = 100-C–H-N-S-ashes. Mineral elemental analysis was carried out after calcination at 450 °C for one day and fusion in Li-metaborate + Li-tetraborate at 1000 °C (Chao and Sanzolone, 1992), followed by ash dissolution with concentrated HNO_3. Element contents were measured by ICP-AES. Element mineralomass was computed from total element contents and rice crop biomass after each cropping period. Phytoliths were extracted from collected rice straws following the procedure of Kelly (1990). Briefly, 2.5 g of dried plant materials (≤1 cm) were digested at 120 °C using a mixed solution of HNO_3 (70%) and H_2O_2 (30%) until the reaction ended (about 10 days). Extracted phytoliths were filtered using a 0.2 μm filter and rinsed with deionized water, oven-dried at 55 °C for 7 days to determine PhSi content.

2.5.3. Leachates

The collected leachates were measured for their volume, filtered on a 0.45 μm filter, and then divided into two aliquots to determine pH and solutes concentrations. The latter extract was kept in darkness at 4 °C prior to further Si, Al, Fe, K, Ca, Na and Mg analyses using ICP-AES.

2.6. Selective Si extractions in soil and soil:biochar mixtures

Around 30 g of soil and soil:biochar mixtures were collected in each individual pot using a small stainless steel auger (2 cm internal diameter, 40 cm length). All samples were air-dried, ground, and sieved at ≤2 mm prior to further analyses.

The Na_2CO_3 extraction of Si is used to quantify biogenic silica in soils (DeMaster, 1981; Koning et al., 2002; Saccone et al., 2007). Briefly, 30 mg of sample was mixed with 40 mL of Na_2CO_3, 0.1 M (pH = 11.2) and digested for 300 min at 85 °C. One ml of extraction solution was sampled at 30, 60, 120, 180, 240, 300 min, then neutralized and acidified using 100 μl of 7 M HNO_3 to measure Si by ICP-AES. The soil biogenic Si content, named here Na_2CO_3-Si, was calculated by determining the intercept of the linear regression at constant extraction rate (DeMaster, 1981; Koning et al., 2002) using the lm function of the R programming language to fit a first-order kinetic model (Cornelis et al., 2011). Starting from the Si + biochar, the impact of dosed additions of tephrite on the extraction of Na_2CO_3-Si was tested by using the same procedure. The five final Si + biochar:tephrite mixtures followed the proportions (%) 100:0, 75:25, 50:50, 25:50 and 0:100.

Dark oxalate (o) selectively dissolves short-range-order (SRO) Si, Al, Fe components in soils (Parfitt et al., 1980; Blakemore et al., 1981; Parfitt and Henmi, 1982; Dahlgren, 1994) whereas *pyrophosphate (p)* (Bascomb, 1968) is routinely used to extract Al- and Fe-humus complexes (Parfitt et al., 1980; Parfitt and Henmi, 1982; Farmer et al., 1983). The procedures compiled by Dahlgren (1994) were used: (i) dark oxalate extraction using 0.2 M ammonium oxalate-oxalic acid at pH 3, followed by analysis of extracted Si_o, Fe_o and Al_o by ICP-AES; (ii) 0.1 M Na pyrophosphate, analysis of extracted Al_p and Fe_p by ICP-AES. We

used Si_o, Al_o and Al_p to compute the Si:Al atomic ratio (Si_o:(Al_o-Al_p)) of allophanic substances.

The $CaCl_2$ extractable Si ($CaCl_2$-Si) is considered as plant available Si in soils (Haysom and Chapman, 1975; Sauer et al., 2006). It was measured through a kinetic extraction method (Li et al., 2019) using a solid:liquid ratio 5 g:50 mL (0.01 M $CaCl_2$) in 100 mL polyethylene cups shaken at 25 °C. The 1:10 solid:liquid ratio was kept constant using replicates for both the extraction and analysis. At each time step (6 h, 12 h, 1 day, 2 days, 4 days, 8 days, 16 days, 32 days, 64 days and 128 days), the collected suspension (50 mL) was centrifuged at 3,000g for 20 min. The supernatant (40 mL) was filtered and separated in two aliquots of 20 mL to measure, respectively, pH and solutes concentrations. The latter extract was acidified by adding 100 µl of HNO_3 7 M, then stored in darkness at 4 °C prior to further analyses.

2.7. Data analyses

Averages, standard deviations of all measured variables, and statistical tests were performed using SPSS 24.0 software. The significance of the difference between measured values among all treatments was measured with Tukey's mean separation test at the $p < 0.05$ level. When average values significantly differ among treatments, they are presented with a different lowercase letter (a, b, c…) (Duncan's notation).

3. Results

3.1. Properties of rice straws (RS), derived biochars, tephrite and albic soil materials

As discussed above, the chemical and mineralogical compositions illustrated in Fig. 1 and Table S1 are typical for albic soil material and fresh tephrite (Fig. S1 and Table S1). Na_2CO_3-Si and $CaCl_2$-Si are negligible in the Podzol albic horizon (0 and 0.03 g kg^{-1}), and low in the tephrite (3.8 and 1.5 g kg^{-1}).

The rice straws Si-RS and Si + RS significantly differ in fresh biomass (31.3 and 40.4 g $plant^{-1}$), dry biomass (5.0 and 7.9 g $plant^{-1}$) and Si content (0.01 and 1.10%) (Table S2). Yet Si-RS and Si + RS did not significantly differ in C, N, H, O, Ca, K, Mg, Na and ash contents, nor in C/N, H/C and O/C ratios.

The Si − and Si + biochars did not significantly differ in C, H, N, Ca, K, Mg and Na contents, C/N, H/C and O/C ratios, and pH-H_2O (Table S2). Si − and Si + biochars significantly differ in yield (31.8 and 38.2%, respectively), their respective contents of O (5.1 and 7.5%) and Si (0.1 and 4.8%), Na_2CO_3-Si (0.1 and 15.6 g kg^{-1}) and $CaCl_2$-Si (0.1 and 15.2 g kg^{-1}). The SEM micrographs and related EDX element mapping confirmed that Si − was free of phytoliths (Fig. 1a, c), while Si + contained dumbbell-shaped and fine silt-sized phytoliths (Fig. 1b, d).

3.2. Soil pH, allophane and ferrihydrite contents in soils and soil:biochars mixtures

In the 5 g:50 mL solid:liquid suspensions, pH-$CaCl_2$ ranged from 3.8 to 5 in tephrite, 7.3 to 10.0 in Si − and Si + biochars (Fig. S3a). In soils, pH-$CaCl_2$ was 3.8–4.0 in T5, 3.9–4.4 in T15, but markedly increased with increasing time from 4.0 to 6.3 in T45, from 4.2 to 6.6 in T135, and from 5.8 to 7.0 in T405 (Fig. S3b; Table S6). The pH-$CaCl_2$ increased with increasing time in all soil:biochar mixtures, with the following respective minimum–maximum values: 4.3–6.4 in Si-T5, 4.6–6.8 in Si-T15, 5.0–7.0 in Si-T45, 5.0–7.1 in Si-T135, 5.5–7.2 in Si-T405, 4.1–5.6 in Si + T5, 4.6–6.8 in Si + T15, 4.5–6.9 in Si + T45, 5.3–7.4 in Si + T135, 5.3–7.7 in Si + T405 (Fig. S3c-d; Table S6). Thus, in soils and soil:biochar mixtures, both minimum and maximum pH values increased with increasing TRB and increasing time, from day 1 to day 128, revealing an increased time-course proton consumption with increasing TRB.

Allophane and ferrihydrite contents, as well as the Si:Al atomic ratio of allophanic substances, were computed from Si_o, Al_o, Al_p and Fe_o concentrations (Tables S3-S5). They revealed the formation of both SRO minerals, and further showed that the range of the Si:Al atomic ratio (0.5–1.0) was typical for the series imogolite-allophane. Allophane did not occur in T5, although its content increased with increasing TRB (Table S3). A similar evolution was observed for ferrihydrite. The contents of SRO minerals in both soils and soil:biochar mixtures significantly increased with increasing time and TRB (Tables S3-S5). The rate of the formation of the allophanic substances also increased with increasing TRB, up to 0.85 g kg^{-1} day^{-1} for TRB = 405 $cmol_c$ kg^{-1} (Fig. 2).

3.3. Na_2CO_3-Si and $CaCl_2$-Si contents in soils and soil:biochars mixtures

The Na_2CO_3-Si and $CaCl_2$-Si contents are determined to assess biogenic silica and plant available Si in soils, respectively (DeMaster, 1981; Sauer et al., 2006). From Tables S1 and S2, Na_2CO_3-Si (g kg^{-1}) is negligible in the albic soil material (0) and Si-biochar (0.12). It amounts to 3.8 g kg^{-1} in tephrite and 15.6 g kg^{-1} in Si + biochar in which $CaCl_2$-Si (g kg^{-1}) accounts for 39 and 97% of Na_2CO_3-Si, respectively, suggesting that the pool of Na_2CO_3-Si is totally bioavailable in Si + biochar. A constant dissolution rate was rapidly attained during the kinetic extraction of Si from tephrite in Na_2CO_3 (Fig. S4a). Yet the clear non-linear part of the dissolution curve could not be attributed to phytogenic silica in the fresh tephrite. Na_2CO_3-Si content linearly decreased with increasing proportion of tephrite in Si + biochar:tephrite mixtures (Fig. S4b). It indeed decreased from 15.6 in pure Si + biochar to 3.8 g kg^{-1} in pure tephrite, confirming that Na_2CO_3 extraction was not specific to biogenic Si, and thus the *DeMaster* technique (DeMaster, 1981) to quantify phytoliths in soils and sediments can be questioned (Meunier et al., 2014; Kaczorek et al., 2019; Li et al., 2019). As illustrated in Fig. S5a, Na_2CO_3-Si was not detected or negligible in T5, T15, Si-T5 and Si-T15, confirming the absence of biogenic silica in the albic material and Si-biochar. It increased with increasing TRB from 0.2 in T45 to 3.2 g kg^{-1} in T405 and 2.4 g kg^{-1} in Si-T405, despite the absence of phytogenic silica in tephrite and Si-biochar (Fig. S5a). The maximum value was observed in Si + T405 (3.7 g kg^{-1}) (Fig. S5a). Similar trends were observed for the 1st and 2nd cropping periods (Fig. S5a-b). The $CaCl_2$ kinetic extractions performed on all materials (Fig. 3) illustrated the ample supply of plant available Si (g kg^{-1}) from Si + biochar (15.6), its virtual absence in Si-biochar (0.11), and a substantial amount in tephrite (1.5) (Fig. 3a). Increasing TRB resulted in increasing $CaCl_2$-Si contents in soils (Fig. 3b-d). However, $CaCl_2$-Si at day 128 (mg kg^{-1}) was larger in soils (from 30 in T5 to 90 in T405) than in Si-biochar:soils (from 20 in Si-T5 to 67 in Si-T405 (67.2) (Fig. 3b-c). Supplying Si + biochar to soils resulted in a significant increase in $CaCl_2$-Si (117.1 mg kg^{-1}). As shown in Fig. 4, $CaCl_2$-Si was significantly larger in bare soils than in rice-cropped soils after both cropping periods. During the 1st cropping period, $CaCl_2$-Si was significantly larger in non-amended soils than in biochar amended soils except in T5 (Fig. 4a). It is clear that the concentration of aqueous $H_4SiO_4^0$ in the $CaCl_2$ invariably decreases from day 0.25 (6 h) to day 128 (Table S6). This concentration at d128, here named $H_4SiO_4^0$-d128, is one order of magnitude larger in Si + biochar ($10^{-3.27}$ M) than in tephrite ($10^{-4.27}$ M), indicating that dissolved Si is controlled by different silica phases, i.e., phytolith in Si + biochar and weatherable lithogenic aluminosilicates in tephrite. In the albic material (T5), $H_4SiO_4^0$-d128 is $10^{-3.92}$ M, suggesting that dissolved Si is controlled by quartz. The increase in TRB resulted in an increase of $H_4SiO_4^0$-d128 from $10^{-3.92}$ to $10^{-3.65}$ M. Supplying Si-biochar to soils gave the same trend, from $10^{-4.20}$ to $10^{-3.62}$ M, whereas supplying Si + biochar increased $H_4SiO_4^0$-d128 from $10^{-3.72}$ to $10^{-3.41}$–$10^{-3.38}$ M, supporting the control of dissolved Si by phytoliths.

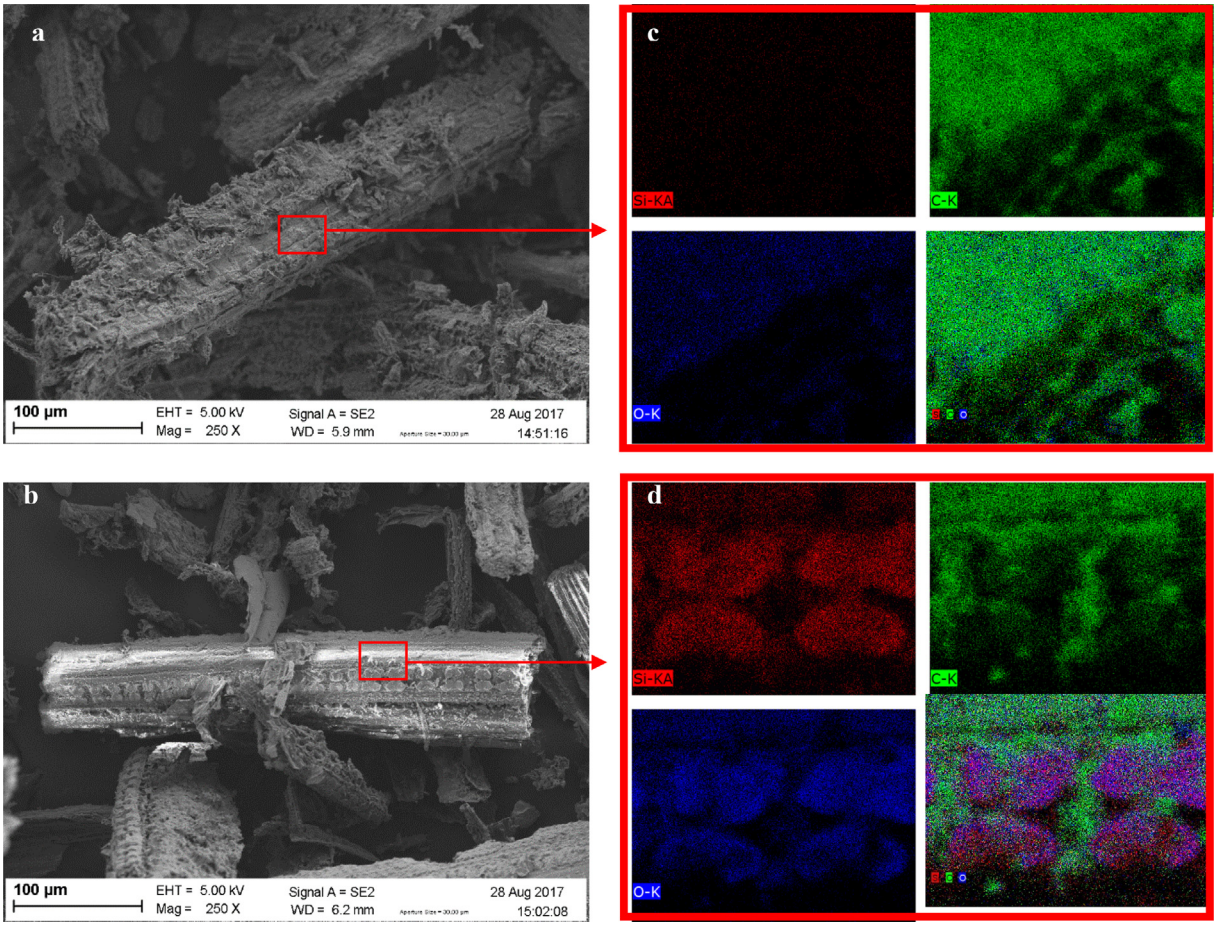

Fig. 1. SEM images of biochar particles in (a) Si− and (b) Si+ biochars. The corresponding EDX spectra maps of elements (Si, C, O) performed on these biochar particles from (c) Si− and (d) Si+, demonstrate the presence of phytoliths in Si+ after pyrolysis.

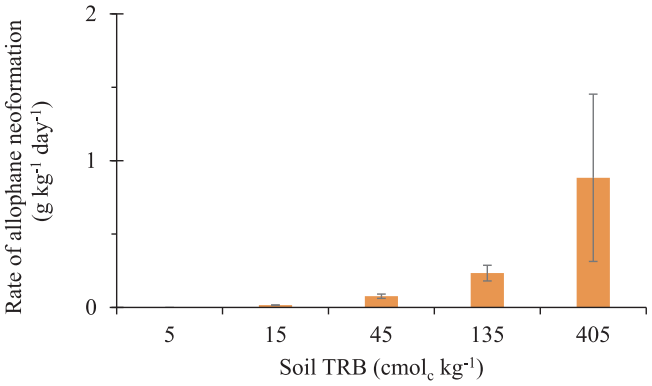

Fig. 2. Rate of allophane neoformation (g kg^{-1} day^{-1}) in the bare soil during the 16 weeks experimental period, calculated from the allophane contents as measured at 4th, 8th, 12th and 16th week.

3.4. Leachate properties

As shown in Fig. 5, pH increased with increasing TRB in soils, from 3.9 in T5 to 7.7–8.7 in T135 or T405, in both cropping periods. Supplying biochar (with or without Si) resulted in a pH increase in all soils, confirming the rapid liming effect of biochar in an un-buffered soil such as T5. In bare soils, leachate DSi was negligible in T5, but increased by eight-fold in T15, and then decreased with increasing TRB. In cropped soils without biochar supply, exported DSi followed the same trend, but the maximum DSi loss (T15) was below that in bare soil in the 1st cropping period (Fig. 5a). Exported DSi was invariably below 10 mg L^{-1} in Si− amended soils and above 20 mg L^{-1} in Si+ amended soils (Fig. 5a). DSi losses through leaching significantly decrease during the 2nd cropping period at given TRB (Fig. 5b); yet, DSi loss regularly increased with increasing TRB. Dissolved Al content (mg L^{-1}) first raised from 1.9 in T5 to 3–4.5 (Fig. 5a) and to 10–25 (Fig. 5b) in T15 or T45. In contrast, exported Al (mg L^{-1}) was much lower in biochar-amended soils, below 2 in the 1st cropping season, and 10 in the 2nd one. Aqueous Fe concentrations in leachate were invariably lowest in soils with high TRB (T135, T405), either amended with biochar or not. In contrast, the highest Fe concentrations were observed in soils with low TRB.

3.5. Si in plants

Plant PhSi content (g kg^{-1}), as assessed by the procedure of Kelly (1990), significantly increased from 4.4 in T5 to 40.8 in T405 in the 1st cropping season, and from 7.48 in T5 to 42.56 in T405 in the 2nd cropping season (Table 1). Similar trends were observed in soils amended with biochar, but with larger plant PhSi content in Si+ soils, up to 58.4 g kg^{-1} in Si+T405 (Table 1). So, plant PhSi content positively responded to TRB and Si+ supply. Since plant dry matter also positively responded to TRB (up to 135 $cmol_c$ kg^{-1}) and Si+ supply, Si mineralomass (mg pot^{-1}) logically increased from 1.5 to 300 with increasing TRB and phytolith supply (Table 1). As inferred from Table 1, in T5 soil, the contribution of biochar-PhSi to plant-PhSi (mg pot^{-1}) thus amounted to (94.6–19.4) = 75.2 in the 1st cropping period (without rice straw return), i.e. 79.5% of plant PhSi. In the same soil, the contribution of biochar-PhSi to plant-PhSi (mg pot^{-1}) amounted to (46.2–15.6) = 30.6 in the 2nd cropping period (with rice straw return),

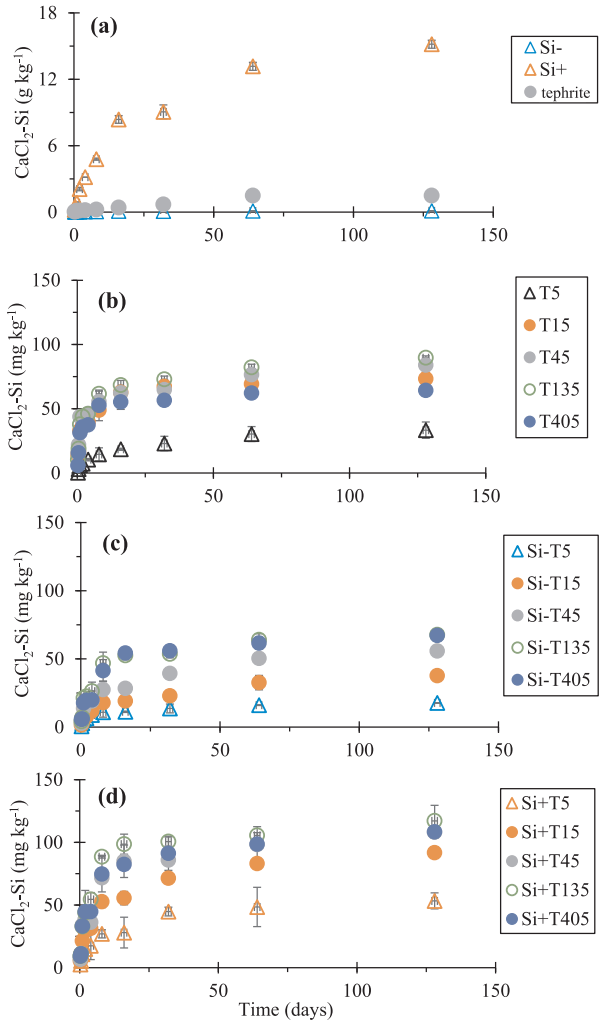

Fig. 3. Plot of the $CaCl_2$ extractable Si content ($CaCl_2$-Si), as assessed prior to the 1st cropping, against time: 6 h, 12 h, 24 h (1 day), 2, 4, 8, 16, 32, 64 and 128 days before the 1st cropping. (a) Si sources: Si-biochar, Si + biochar and tephrite. (b) Soils; (c) Si-biochar:soils; (d) Si + biochar:soils. In soils and biochar:soil mixtures, the albic material was mixed with fresh powdered tephrite to reach the respective TRB values (5, 15, 45, 135 and 405 $cmol_c\ kg^{-1}$). Note that the units of $CaCl_2$-Si are in g kg^{-1} in (a), but mg kg^{-1} in (b-d).

i.e. 66.2% of plant PhSi.

4. Discussion

4.1. Si sources in the experimental soil–plant system

The absence of PhSi in the albic soil material (Table S1) reveals the very poor biological activity in Podzol subsurface horizons, which involves the accumulation of organic matter (litter and partly decomposed litter) and the lack of bioturbation. These well-known processes in Podzols explain the absence of phytoliths in the bleached E horizon. Indeed, the phytolith pool in forest soils is supplied from falling litter debris in organic horizons (Bartoli, 1983; Alexandre et al., 1997; Meunier et al., 1999; Gérard et al., 2008; Cornelis et al., 2011; Sommer et al., 2013), which are not mixed with mineral horizons beneath the E horizon in Podzols. On the other hand, this pool is the main source of plant-available Si in highly weathered soils (Lucas et al., 1993; Henriet et al., 2008b; Cornelis and Delvaux, 2016). Not surprisingly, Na_2CO_3-Si and $CaCl_2$-Si contents are thus negligible in the albic soil material (Table S1). Fresh tephrite contains a number of weatherable lithogenic aluminosilicates that may rapidly dissolve, for example olivine and other ferromagnesian silicates, as well as the feldspathoids (leucite and nepheline). Obviously, these lithogenic aluminosilicates release aqueous $H_4SiO_4^0$ in the Na_2CO_3 and $CaCl_2$ extracts. This observation means that the *DeMaster* technique (DeMaster, 1981) to quantify biogenic silica is invalid in soils and corroborates alternative methods (Meunier et al., 2014; Li et al., 2019). In other words, our data show that Na_2CO_3-Si is not biogenic in the tephrite used here as a Si source. In contrast, Na_2CO_3-Si is fully biogenic in Si + since this biochar is derived from pyrolyzed rice straws produced alongside an ample supply of plant available Si (Li et al., 2019). The concentration of aqueous $H_4SiO_4^0$ in $CaCl_2$ extracts at day 128 supports the notion that phytoliths in Si + biochar directly control the $H_4SiO_4^0$ in solution because it is one order of magnitude higher in phytolithic biochar ($10^{-3.27}$ M) than in tephrite ($10^{-4.27}$ M) (Table S6 and Fig. S8). Our experimental data evidently show that both tephrite and Si + biochar release available Si for plant uptake since both sources significantly increase the plant PhSi content (Table 1), the PhSi silicate being the main contributor in the absence of lithogenic aluminosilicates (Table 1). Through an *in vitro* controlled experimental soil–plant system, we first demonstrated that the primary source of plant-available Si in soils is the reserve of weatherable lithogenic aluminosilicates (Henriet et al., 2008a; Klotzbücher et al., 2015). Then, we showed that the soil PhSi pool takes over the lithogenic aluminosilicate reserve in highly weathered soils, as suggested earlier from meta-analyses of field data gathered worldwide (Cornelis and Delvaux, 2016; Vander Linden and Delvaux, 2019).

As far as Si − and Si + biochars are concerned, Si-biochar does not significantly increase the phytogenic Si pool in any soil, whatever its TRB, confirming that Si-biochar is depleted in Si. In contrast, Si + biochar is a major supplier of phytogenic silica. Surprisingly, the return of rice straws into soil prior to the 2nd cropping period does not significantly increase the plant PhSi mineralomass, except in Si-T15 and Si + T405 (Table 1). In contrast, the plant PhSi mineralomass decreases in Si-T405, Si + T5, Si + T15, Si + T45, Si + T135, probably because of differences in Si accessibility linked to rice straw decomposition rate in our experimental device.

4.2. Rapid neoformation of aluminous allophanic substances

The pedogenic neoformation of allophanic substances, in particular imogolite, is well known in podzolic environments (Farmer, 1982; Farmer et al., 1983). Allophane has a Si:Al atomic ratio generally ranging from 1 to 2. Here, the allophanic substances are evidently aluminous since their Si:Al atomic ratio ranges from 1 to 0.5, typical for the series allophane-imogolite (Parfitt et al., 1980; Parfitt and Henmi, 1982; Farmer et al., 1983; Parfitt et al., 1983; Bartoli et al., 2007; Parfitt, 2009; Churchman and Lowe, 2012). Our experimental data showing that allophane content increases significantly with increasing TRB is in accordance with the formation of allophanic substances in less weathered Podzol B horizons (Farmer, 1982). In this respect, the tephrite weatherable lithogenic aluminosilicates evidently act as a source for allophane formation in the soils we studied. In fact, the increase in pH as well as the increase in allophane content with increasing TRB show that mineral weathering is an active process in the T15-T405 soils. The combination of lithogenic aluminosilicate dissolution and pedogenic aluminosilicate formation consumes protons (Kittrick, 1977) and thus explains the large increase in pH in non-amended soils (Fig. 5). In this regard, the pH increase linked to the liming effect of biochars might have decreased lithogenic aluminosilicate dissolution. Our experimental device does not allow, however, to infer the possible role of phytolith as a source for allophanic Si. Yet our experimental data shows that allophanic substances form rapidly, at a maximum rate of 0.85 g kg^{-1} day^{-1}, and are a major sink of Si in our controlled soil–plant system. Parfitt (2009) reported that allophane has been observed to precipitate in a matter of months on the face of open soil pits containing rhyolitic tephra.

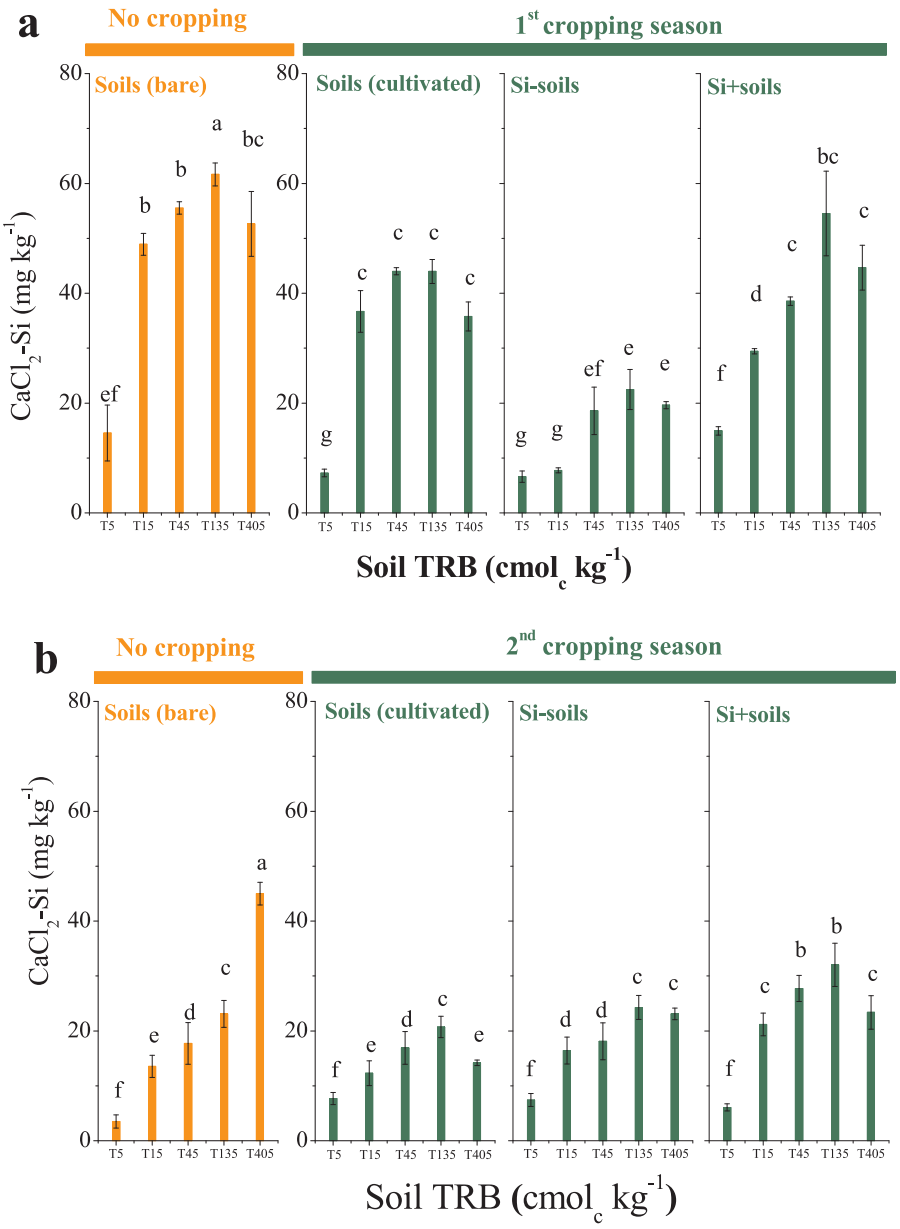

Fig. 4. $CaCl_2$ extractable Si content ($CaCl_2$-Si, mg kg^{-1}) over 12-hour extraction after the (a) 1st cropping and (b) 2nd cropping periods in bare soils, and in cultivated soils mixed with biochars Si− and Si+. The average contents of $CaCl_2$-Si with different lowercase significantly differed at $p < 0.05$ level.

4.3. Si bioavailability and DSi fate in the experimental soil–plant system

As discussed above, the tephrite-lithogenic aluminosilicates and PhSi from Si + biochar are the exclusive sources of plant available Si during the 1st cropping period. In the 2nd cropping period, the return of rice straws results in a significant increase of $CaCl_2$-Si (Fig. S7), and thus consists of an additional source of plant available Si. Numerous previous studies document that soil lithogenic aluminosilicates and PhSi release DSi that supplies the pool of plant available Si (McKeague and Cline, 1963c; Henriet et al., 2008b; Li and Delvaux, 2019; Li et al., 2019). As already mentioned, phytoliths readily dissolve and release bioavailable Si (Fraysse et al., 2006, 2009; Li et al., 2019). Most of the basaltic lithogenic aluminosilicates quickly release DSi (Eggleton et al., 1987; Gislason and Oelkers, 2003; Gudbrandsson et al., 2011). As illustrated in Fig. 3a, $CaCl_2$-Si released from the tephrite sharply increased from 30 mg kg^{-1} after 6 h to 120 mg kg^{-1} after 24 h, and then up to 1490 g kg^{-1} after 128 days of $CaCl_2$ kinetic extraction. We attribute the release of plant-available Si to easily weatherable lithogenic aluminosilicates amounting to 3.82 g Si kg^{-1}, as quantified by the kinetic Na_2CO_3 extraction. In this view, the pool of bioavailable $CaCl_2$-Si would represent 39% of Na_2CO_3-Si. However, the dissolution rate of the basic rock is pH-dependent; this rate first decreases dramatically with pH increasing from pH 2 to 7, then increases slowly from pH 7 to 11 (Gislason and Oelkers, 2003; Gudbrandsson et al., 2011). Here, no clear pattern could be detected to explain the pH-dependency of $CaCl_2$-Si content (Fig. 6b), apart from the inputs of lithogenic aluminosilicates (TRB) and PhSi (biochar), as discussed above. Indeed, $CaCl_2$-Si content does not increase above 125 mg kg^{-1} following a further increase of Na_2CO_3-Si (Fig. 6a), probably because DSi can be retrieved through leaching, plant uptake, adsorption on pedogenic aluminosilicates and/or Al/Fe oxides, and allophane formation. The last process (i.e. allophane formation) is documented above through the formation of allophanic substances. In addition, part of DSi might have been adsorbed onto allophane and/or ferrihydrite surfaces (Delstanche et al., 2009)

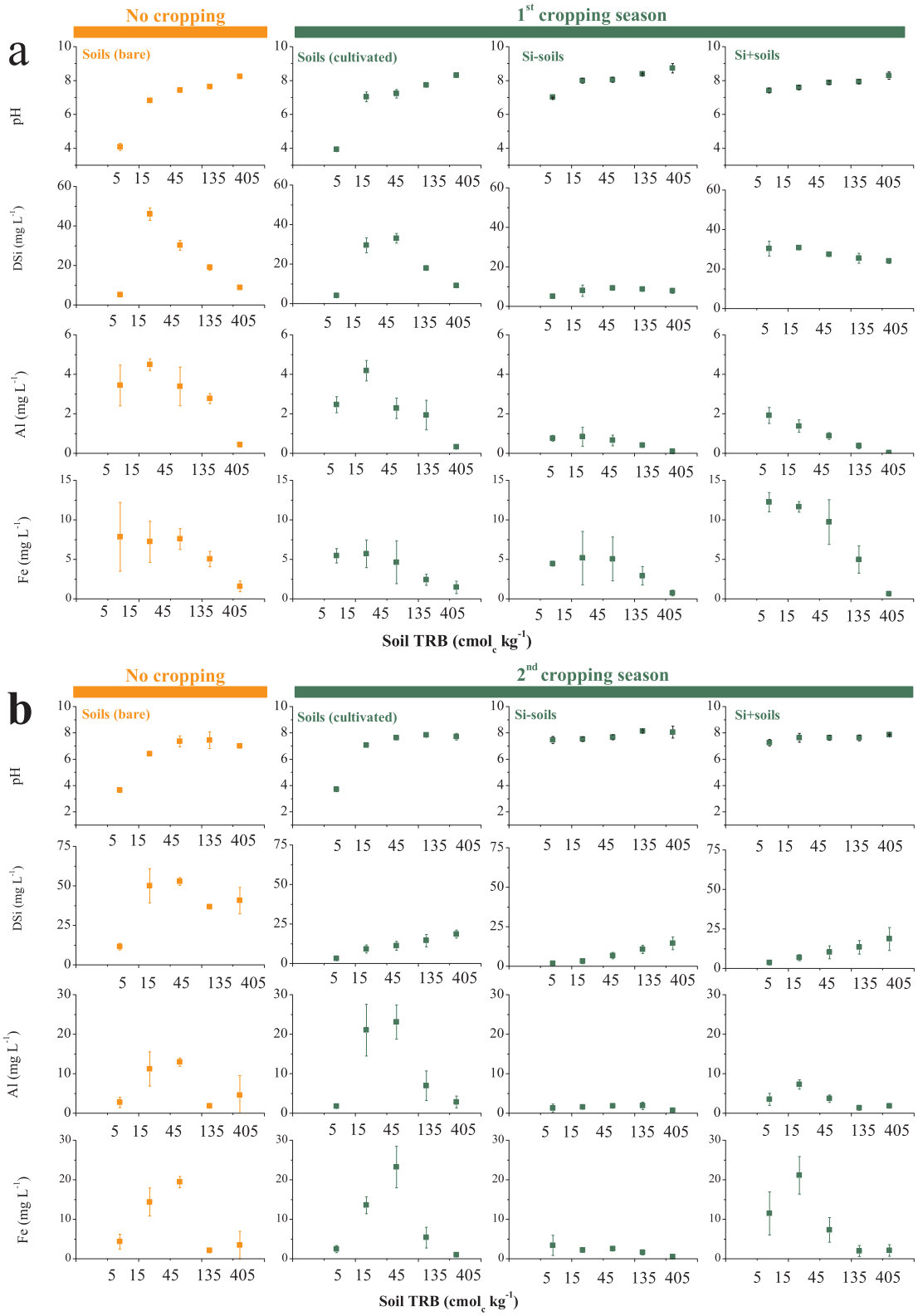

Fig. 5. pH, concentration (mg L^{-1}) of dissolved Si, Al and Fe in the leachates at the 1st cropping and 2nd cropping periods, as collected from bare soils, and cultivated soils non-amended, and mixed with Si− or Si+ biochars.

(Fig. 6c-d), as suggested by the slight decrease of $CaCl_2$-Si for allophane and ferrihydrite contents above 40 g kg^{-1} (Fig. 6c) and 1 g kg^{-1} (Fig. 6d), respectively. On the other hand, Si plant uptake is an important process in our system, directly depending on the pool of plant available Si, as assessed by $CaCl_2$ extraction (Fig. 7). Thus, here, the importance of the processes of Si plant uptake, allophane formation and possibly DSi adsorption explain together the very low exportation of aqueous $H_4SiO_4^0$ through the leachates. Indeed, the loss of DSi through this last route (i.e. DSi leaching) is negligible except in bare soils.

Table 1
Plant shoot dry weight (g pot^{-1}), PhSi (g kg^{-1}) and Si mineralomass (mg pot^{-1}) in harvested rice straws after the 1st and 2nd cropping periods for soils, respectively non-amended, mixed with Si− and Si+ biochars. The average values with different lowercase letters significantly differed at the $p < 0.05$ level of confidence according to Tukey's multiple comparison test.

	1st cropping period			2nd cropping period		
	Plant shoot	PhSi in RS		Plant shoot	PhSi in RS	
	dry weight g pot^{-1}	content g kg^{-1}	mineralomass mg pot^{-1}	dry weight g pot^{-1}	content g kg^{-1}	mineralomass mg pot^{-1}
Soils						
T5	1.07d	4.41 h	4.74 h	0.21e	7.48 g	1.54i
T15	4.90bc	28.01ef	137.29d	2.07d	18.46f	38.29 g
T45	5.02bc	28.05ef	140.74d	2.00d	23.24e	46.40 g
T135	5.16ab	32.49de	167.64c	1.92d	28.48d	54.74f
T405	3.88bc	40.86bc	158.53c	1.60d	42.56b	68.02f
Si-soils						
Si-T5	3.99bc	4.86 h	19.38 g	6.17a	2.53 h	15.62 h
Si-T15	4.18ab	9.27 g	38.78f	4.62bc	18.56f	85.78d
Si-T45	4.82ab	19.49 fg	93.92e	4.06bc	24.21e	98.31d
Si-T135	5.17ab	21.34ef	110.42e	4.12bc	27.71d	114.20d
Si-T405	3.48bc	43.87bc	152.85c	3.14c	43. 88b	137.81c
Si+soils						
Si+T5	4.98ab	18.98f	94.60e	6.30a	7.34 g	46.24 g
Si+T15	5.20ab	36.21 cd	188.39c	4.33bc	19.98f	86.47e
Si+T45	5.54ab	36.79 cd	203.70b	5.62ab	28.84d	162.12b
Si+T135	5.25ab	48.84ab	256.41a	5.24b	35.87c	187.78b
Si+T405	3.55bc	58.44a	207.62b	5.86ab	51.22a	300.13a

4.4. Distribution of Si in the reservoirs of the soil–plant system

The distribution of Si in the different pools is presented in Tables 2 and 3 for the 1st and 2nd cropping period, respectively. The same distribution is illustrated in Fig. 8. To facilitate the understanding of the balances, the distribution of Si is expressed in terms of Si quantities (g or mg pot^{-1}), not concentrations. Fig. 8 is particularly illustrative. It shows that, with or without biochar, the allophanic Si sink remarkably increases with TRB, i.e., the reserve of weatherable lithogenic Si, up to similar values in the range 11.5–14.3 g pot^{-1}. Besides, the allophanic Si

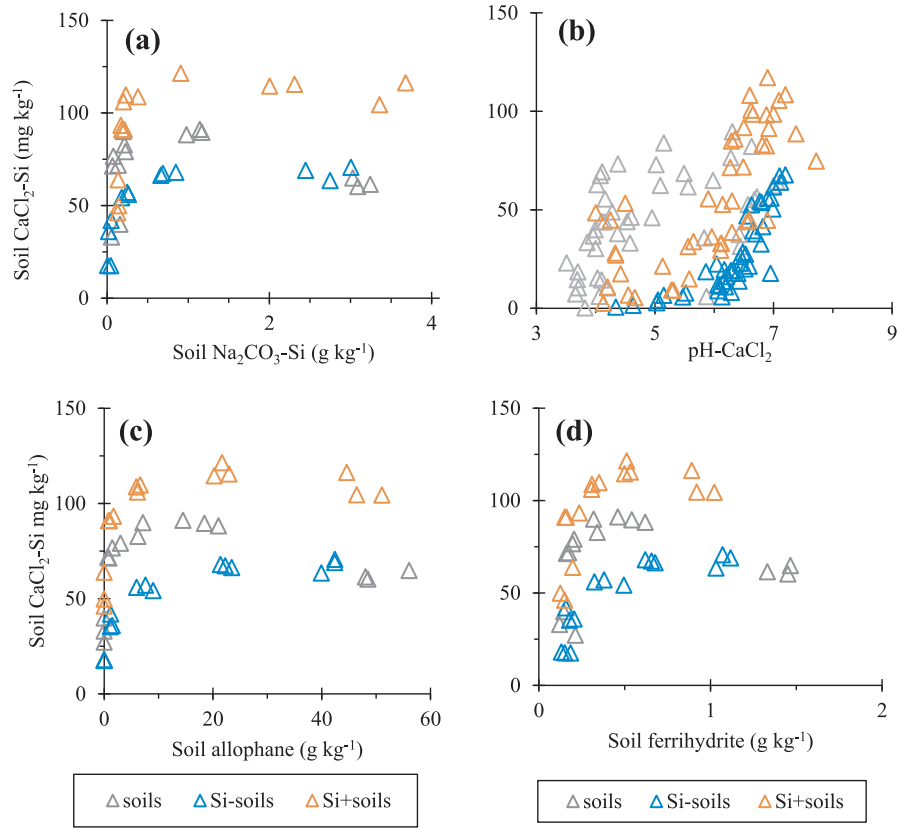

Fig. 6. Plot of $CaCl_2$-Si content against (a) soil Na_2CO_3-Si content, (b) pH-$CaCl_2$ of the extract, (c) allophane and (d) ferrihydrite contents in soil. All contents were measured at harvesting time after the 1st cropping season except for (b) where all data from $CaCl_2$ extracts at 128d were used (after 1st and 2nd cropping seasons).

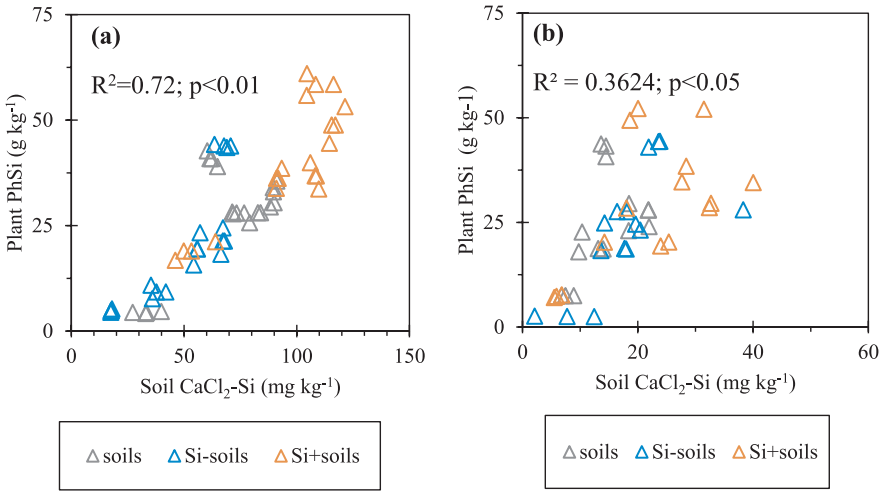

Fig. 7. Plots of plant PhSi content in rice-straw, as assessed following Kelly (1990), against soil $CaCl_2$-Si. (a): after the 1st cropping period; (b) after the 2nd cropping period.

sink significantly competes with the plant phytolith Si sink, given the huge difference in order of magnitude. The largest content of allophanic Si indeed amounts to 14.5 g pot^{-1}, i.e., 48 times above the largest plant PhSi content that reaches 0.3 g pot^{-1}.

In soils and Si-biochar:soil mixtures, leachate DSi accounts for less than 0.03% of the initial lithogenic Si input, whatever the cropping period. DSi loss in the system through leaching is thus negligible, likely because DSi is rapidly involved in allophane neoformation and/or root uptake. Allophanic Si represents 7.0 to 14.1% and 5.3 to 12.4% of initial lithogenic Si input during the first and second cropping period, respectively. Considering the two cropping periods, plant PhSi at harvest accounts for 0.02 to 3.4% of initial lithogenic Si input. In Si + biochar:soil mixtures, leachate DSi accounts for 0.9% in Si + biochar: T5 mixture during the 1st cropping period. In all other Si + biochar:soil mixtures, leachate DSi represents less than 0.05% of initial lithogenic Si input, and thus much less than 0.05% of initial (lithogenic Si + PhSi) input. Thus in Si + biochar:soil mixtures, DSi loss in the system through leaching is also negligible. The two major Si sinks are also allophane and plant phytoliths. Allophanic Si accounts for 8.0–12.4% and 10.3–12.3% of initial lithogenic Si input during the first and second

Table 2
1st cropping period: amounts of the different Si forms in the various reservoirs of the soil–plant system: initial inputs of lithogenic Si and biochar-PhSi, before cropping; final amounts (harvesting time after the 1st cropping period) of plant phytolithic Si, and soil $CaCl_2$-Si, Na_2CO_3-Si, allophanic Si and leachate DSi.

	Soils	Initial lithogenic Si input[1] g pot^{-1}	Initial PhSi input[2] mg pot^{-1}	Plant PhSi at harvest[3] mg pot^{-1}	Soil $CaCl_2$-Si[4] mg pot^{-1}	Na_2CO_3-Si[5] g pot^{-1}	allophanic Si[6] g pot^{-1}	Leachate DSi[7] mg pot^{-1}
Soils (bare)	T5	0	0		10.43	0.00	0.00	0.46
bare	T15	4	0	0	48.91	0.00	0.49	6.89
	T45	15	0	0	55.51	0.23	2.08	3.41
	T135	49	0	0	61.64	1.99	5.46	1.90
	T405	153	0	0	52.62	6.04	11.46	0.95
Soils (cultivated)								
cultivated	T5	0	0	4.74	7.27	0.00	0.00	0.41
	T15	4	0	137.29	36.69	0.00	0.28	2.56
	T45	15	0	140.74	44.01	0.23	1.53	1.89
	T135	49	0	167.64	43.96	1.99	5.06	1.92
	T405	153	0	158.53	35.79	6.04	14.33	0.54
Si-soils								
cultivated	Si-T5	0	6.5	19.38	6.58	0.00	0.00	0.65
	Si-T15	4	6.5	38.78	7.75	0.00	0.36	0.96
	Si-T45	15	6.5	93.92	18.57	0.26	2.12	1.28
	Si-T135	49	6.5	110.42	22.49	1.27	6.30	0.66
	Si-T405	153	6.5	152.85	19.63	5.27	11.71	0.67
Si + soils								
cultivated	Si + T5	0	241	94.60	14.92	0.07	0.00	2.12
	Si + T15	4	241	188.39	29.41	0.13	0.32	2.22
	Si + T45	15	241	203.70	38.55	0.34	1.75	3.10
	Si + T135	49	241	256.41	54.50	3.28	6.09	2.34
	Si + T405	153	241	207.62	44.65	7.40	13.34	0.83

[1] Initial lithogenic Si input from tephrite supply.
[2] Initial PhSi input from biochar.
[3] Final amount of phytolithic Si in rice straws, as assessed from Kelly (1990).
[4] Final amount of $CaCl_2$ extractable Si in soil.
[5] Na_2CO_3-Si: amount inferred from the method of DeMaster (1981).
[6] Si amount computed from Si_o content.
[7] Final amounts of DSi in leachate.

Table 3
2nd cropping period: amounts of the different Si forms in the various reservoirs of the soil–plant system: initial inputs of lithogenic Si and biochar-PhSi, before the 2nd cropping; final amounts (harvesting time after the 2nd cropping period) of plant phytolithic Si, and soil $CaCl_2$-Si, Na_2CO_3-Si, allophanic Si and leachate DSi.

	Soils	Initial lithogenic Si reserve[1] g pot^{-1}	Initial PhSi input[2] mg pot^{-1}	Plant PhSi at harvest[3] mg pot^{-1}	Soil $CaCl_2$-Si[4] mg pot^{-1}	Na_2CO_3-Si[5] g pot^{-1}	allophanic Si[6] g pot^{-1}	Leachate DSi[7] mg pot^{-1}
Soils bare	T5	0.00	0		7.03	0.00	0.00	0.65
	T15	3.75	0	0	27.10	0.00	0.25	6.22
	T45	13.44	0	0	35.42	0.23	1.56	5.68
	T135	43.92	0	0	46.21	1.99	5.08	5.37
	T405	139.73	0	0	90.00	6.04	13.27	2.78
Soils cultivated	T5	0.00	0	1.54	15.38	0.00	0.00	0.33
	T15	3.80	0	38.29	24.58	0.00	0.20	0.63
	T45	13.56	0	46.40	33.80	0.23	1.44	0.80
	T135	44.25	0	54.74	41.41	1.99	4.75	1.55
	T405	140.77	0	68.02	28.38	6.04	12.23	1.11
Si-soils cultivated	Si-T5	0.00	13.40	15.62	14.84	0.01	0.00	0.21
	Si-T15	3.65	30.60	85.78	32.85	0.03	0.35	0.37
	Si-T45	13.34	64.30	98.31	36,19	0.32	1.66	0.95
	Si-T135	43.99	70.43	114.20	48.55	1.34	5.01	1.21
	Si-T405	138.62	144.78	137.81	46.22	5.41	14.38	0.79
Si + soils cultivated	Si + T5	0.00	56.60	46.24	12.13	0.13	0.04	0.25
	Si + T15	3.63	97.78	86.47	42.37	0.23	0.37	0.46
	Si + T45	13.36	93.81	162.12	55.43	0.44	1.64	1.18
	Si + T135	44.42	132.00	187.78	64.04	3.41	4.58	1.25
	Si + T405	138.45	156.04	300.13	46.75	7.56	14.55	0.65

[1] Lithogenic Si reserve after 1st cropping, but before 2nd cropping.
[2] Phytolithic Si supply to soil from the return of rice straws harvested from the 1st cropping period.
[3] Final amount of phytolithic Si in rice straws, as assessed from Kelly (1990).
[4] Final amount of $CaCl_2$ extractable Si in soil.
[5] Na_2CO_3-Si: amount inferred from the method of DeMaster (1981).
[6] Si amount computed from Si_o content.
[7] Final amounts of DSi in leachate.

cropping periods, respectively. Since the allophanic substances are in the allophane-imogolite range, we hypothesize that they form in mineral microenvironments rich in Al (Farmer, 1982; Eggleton et al., 1987), thus in weathering solutions close to dissolving lithogenic aluminosilicates, and not around phytolith particles. Following this line of reasoning, phytoliths, as released through biochar and/or rice straw supply, would not contribute to allophane formation. The similarity of allophane contents in soils, Si-biochar:soil and Si + biochar:soil mixtures, as well as the rather homogenous ratio [allophanic Si: lithogenic Si], support this hypothesis. In Si + biochar:soil mixtures, the plant PhSi amount originates from tephrite-lithogenic Si and biochar-PhSi in the 1st cropping period, and from these two sources added to the PhSi contribution from RS returned to soil. It is, however, possible to quantify the proportions of plant PhSi originating from lithogenic Si and PhSi (biochar or rice straw) by deducting the respective plant PhSi amounts in Si-biochar:soil mixtures from the respective plant PhSi amounts in Si + biochar:soil mixtures, using the former mixtures as control (see next section).

4.5. Respective contributions of soil lithogenic Si and PhSi to the plant PhSi reservoir

As proposed above, the respective proportions of plant PhSi originating from lithogenic Si and PhSi are presented in Table 4. In the first cropping period, the contribution of PhSi supply accounts for 80% in the most weathered soil T5. With increasing TRB, hence lithogenic Si reserve, the PhSi contribution progressively decreases to 26%. In other words, with increasing weathering stage, the phytolith pool in soil takes over of the mineral one to provide plant available Si. This observation is confirmed in the 2nd cropping period, but to a lesser extent, probably because of the return of rice straws into soil prior to the 2nd cropping.

Our experimental data thus demonstrate three facts about the interactions between the mineral Si contribution to plant-available Si and biological Si feedback loop in the soil–plant cycle of Si. (1) The mineral Si contribution is particularly active once weatherable minerals readily dissolve to provide plant-available Si and supply DSi for allophane formation. (2) With increasing soil weathering stage, the biological feedback loop takes over the mineral contribution to plant available Si. (3) Even in less weathered soils, phytoliths can be very competitive to supply plant-available Si. Thus, despite of the major mineral Si sink consisting of neoformed pedogenic aluminosilicates (here allophane), the contribution of soil phytoliths to plant Si accumulation can be largely above 50% because of their fast rate of dissolution (Fraysse et al., 2006, 2009; Li et al., 2019), and reach 80–90% once the reserve in weatherable lithogenic aluminosilicates is exhausted. This means that, in highly weathered soils, phytolith supply through returning crop residues or supplying phytolith-rich biochar can alleviate natural soil desilication. Our results thus corroborate previous field studies (Bartoli, 1983; Lucas et al., 1993; Alexandre et al., 1997; Meunier et al., 1999; Gérard et al., 2008; Henriet et al., 2008a; Klotzbücher et al., 2016; Marxen et al., 2016). They further validate, on an experimental basis, the interpretative model proposed by Cornelis and Delvaux (2016) about the reciprocal balances between the mineral contribution to DSi and biological Si feedback loop in the soil–plant cycle of Si (Vander Linden and Delvaux, 2019). In this respect, we further conclude that phytolithic biochar boosts the biological Si feedback loop in soil–plant systems by increasing Si bioavailability, which may further depend on soil properties and processes, hence soil type.

5. Conclusion

We set up a controlled soil–plant-solution experiment using a soil

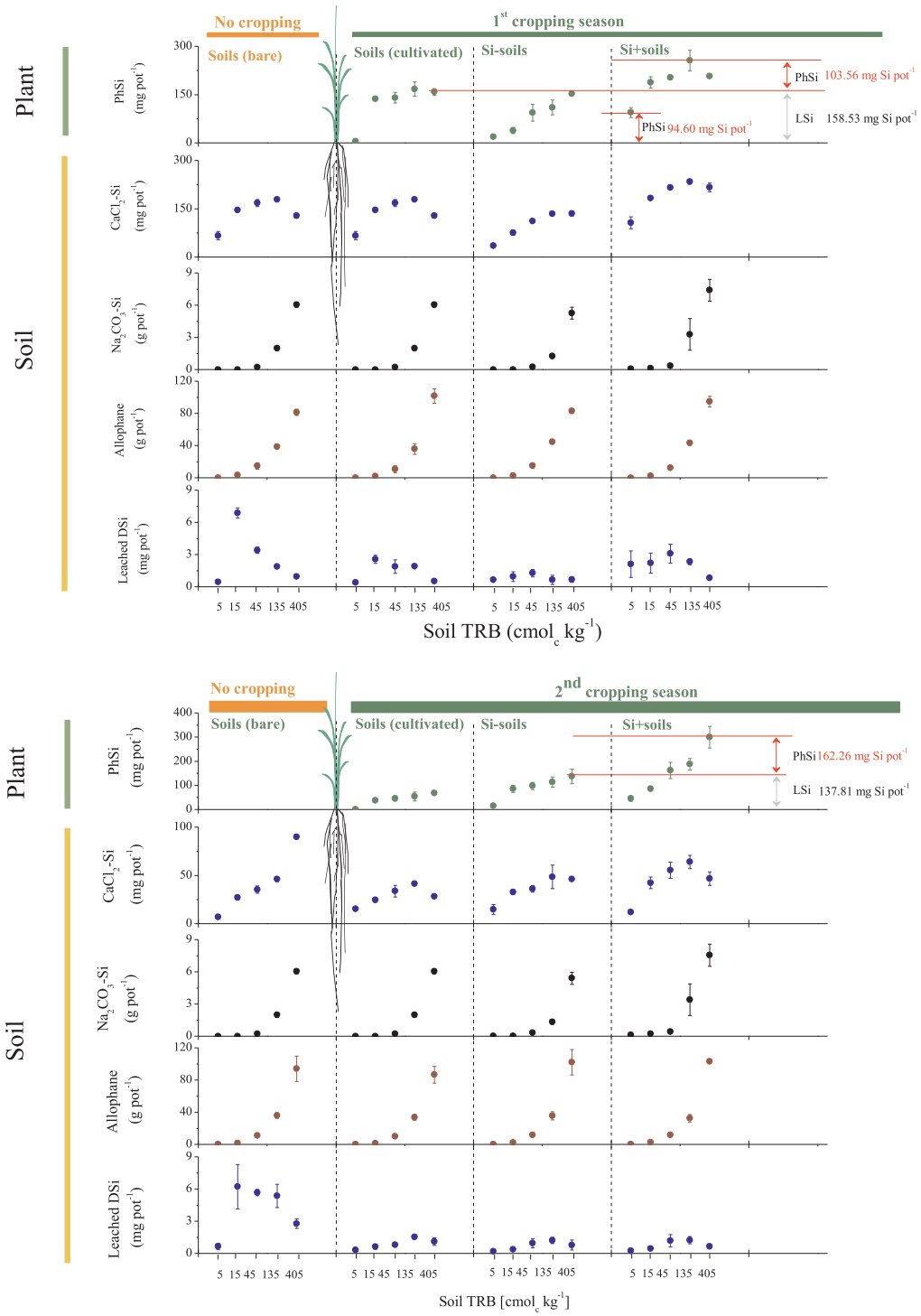

Fig. 8. Amounts (g or mg pot^{-1}) of the different Si forms in the various reservoirs of the soil–plant system: plant PhSi, soil $CaCl_2$-Si, Na_2CO_3-Si, allophane and leachate DSi. Note: lithogenic Si (LSi).

material containing no weatherable silicates and phytoliths, and rice plant for two successive cropping periods. We controlled the Si supply to soil by dosed additions of fresh powdered tephrite and known additions of phytoliths, and we determined the amounts of Si in the pools of the soil–plant cycle of Si. It was shown that, in this cycle, the mineral Si contribution to plant available Si and the biological Si feedback loop were mutually competitive. The weatherable lithogenic aluminosilicates rapidly dissolved and released Si for plant uptake (< 3%) and for recombination with Al to form aluminous allophanic substances (> 50%). The amounts of these allophanic substances were similar irrespective of the cropping period and phytolith supply. Both the amounts of allophane and plant phytolith increased with increasing supply of weatherable lithogenic aluminosilicates, but allophane was, by far, the largest Si sink. Supplying PhSi through the addition of phytolithic biochar largely enhanced the biological Si feedback loop by increasing plant available Si. Yet, at identical phytolith supply, Si bioavailability largely depended on soil weathering stage.

Table 4
Contribution of PhSi from Si + biochar and rice straw supply to the plant PhSi amount for the two cropping periods.

Biochar:soils mixtures	Contribution of PhSi supply to the plant PhSi amount[1]	
	%	
	1st cropping period	2nd cropping period
Si-soils		
Si-T5		90
Si-T15		55
Si-T45		53
Si-T135		52
Si-T405		51
Si + soils		
Si + T5	80	97
Si + T15	79	56
Si + T45	54	71
Si + T135	56	71
Si + T405	26	77

[1] At given lithogenic Si amount (i.e. TRB level), PhSi plant accumulation (the calculated mass balance) is hypothesized to be equal in cultivated soils not amended and amended with phytolith depleted in biochar, assuming that the lithogenic Si contribution to plant uptake is not driven by plant biomass. The contribution of lithogenic Si to the plant PhSi amount is thus obtained by subtraction from 100%.

Acknowledgements

We thank A. Iserentant and C. Givron for laboratory assistance (UCLouvain), and T. Dagbert for technical advice (UCLouvain), as well as Prof. F. Ronsse and Mr. M. Pala for biochar preparation (Ghent University). Z. Li is supported by the 'Fonds Spécial de Recherche' of the UCLouvain in 2014-2015 and the Aspirant (ASP) - 'Fonds National de la Recherche Scientifique' (FNRS) and Chargé de recherches (CR)- FNRS of Belgium. All authors contributed to paper writing and revision. The authors have declared no conflict of interest.

Appendix A. Supplementary data

Supplementary data to this article can be found online at https://doi.org/10.1016/j.geoderma.2020.114308.

References

Alexandre, A., Meunier, J.-D., Colin, F., Koud, J.-M., 1997. Plant impact on the biogeochemical cycle of silicon and related weathering processes. Geochim. Cosmochim. Acta 61, 677–682.
Bartoli, F., 1983. The biogeochemical cycle of silicon in two temperate forest ecosystems. Ecol. Bull. 469–476.
Bartoli, F., Burtin, G., Herbillon, A., 1991. Disaggregation and clay dispersion of Oxisols: Na resin, a recommended methodology. Geoderma 49, 301–317.
Bartoli, F., Poulenard, A., Schouller, B., 2007. Influence of allophane and organic matter contents on surface properties of Andosols. Eur. J. Soil Sci. 58, 450–464.
Bascomb, C., 1968. Distribution of pyrophosphate-extractable iron and organic carbon in soils of various groups. J. Soil Sci. 19, 251–268.
Beckwith, R., Reeve, R., 1963. Studies on soluble silica in soils. I. The sorption of silicic acid by soils and minerals. Soil Res. 1, 157–168.
Belanger, R.R., 1995. Soluble silicon: its role in crop and disease management of greenhouse crops. Plant Dis. 79, 329–336.
Blakemore, L., Searle, P., Daly, B., 1981. Soil Bureau Laboratory Methods. A: Methods for chemical analysis of soils. Newland Soil Bureau Scientific Report 10 A. CSIRO, Lower Hutt, New Zealand.
Carey, J.C., Fulweiler, R.W., 2012. The terrestrial silica pump. PLoS One 7, e52932.
Chao, T., Sanzolone, R., 1992. Decomposition techniques. J. Geochem. Explor. 44, 65–106.
Chapman, H., 1965. Cation-exchange capacity. Methods of soil analysis. Part 2. Chemical and microbiological properties, 891-901.
Churchman, G.J., Lowe, D.J., 2012. Alteration, Formation, And Occurrence of Minerals in Soils. CRC Press (Taylor & Francis), Boca, Raton, FL.
Cornelis, J.-T., Titeux, H., Ranger, J., Delvaux, B., 2011. Identification and distribution of the readily soluble silicon pool in a temperate forest soil below three distinct tree species. Plant Soil 342, 369–378.
Cornelis, J.T., Delvaux, B., 2016. Soil processes drive the biological silicon feedback loop. Funct. Ecol. 30, 1298–1310.
Crane-Droesch, A., Abiven, S., Jeffery, S., Torn, M.S., 2013. Heterogeneous global crop yield response to biochar: a meta-regression analysis. Environ. Res. Lett. 8, 044049.
Dahlgren, R., 1994. Quantification of allophane and imogolite. Quant. Methods Soil Mineral. 430–451.
Delstanche, S., Opfergelt, S., Cardinal, D., Elsass, F., André, L., Delvaux, B., 2009. Silicon isotopic fractionation during adsorption of aqueous monosilicic acid onto iron oxide. Geochim. Cosmochim. Acta 73, 923–934.
Delvaux, B., Herbillon, A.J., Vielvoye, L., 1989. Characterization of a weathering sequence of soils derived from volcanic ash in Cameroon. Taxonomic, mineralogical and agronomic implications. Geoderma 45, 375–388.
DeMaster, D.J., 1981. The supply and accumulation of silica in the marine environment. Geochim. Cosmochim. Acta 45, 1715–1732.
Eggleton, R.A., Foudoulis, C., Varkevisser, D., 1987. Weathering of basalt: changes in rock chemistry and mineralogy. Clays Clay Minerals 35, 161–169.
Epstein, E., 1994. The anomaly of silicon in plant biology. Proc. Natl. Acad. Sci. 91, 11–17.
Exley, C., 1998. Silicon in life: a bioinorganic solution to bioorganic essentiality. J. Inorg. Biochem. 69, 139–144.
Farmer, V., 1982. Significance of the presence of allophane and imogolite in podzol Bs horizons for podzolization mechanisms: a review. Soil Science Plant Nutrit. 28, 571–578.
Farmer, V., Delbos, E., Miller, J., 2005. The role of phytolith formation and dissolution in controlling concentrations of silica in soil solutions and streams. Geoderma 127, 71–79.
Farmer, V., Russell, J., Smith, B., 1983. Extraction of inorganic forms of translocated Al, Fe and Si from a podzol Bs horizon. J. Soil Sci. 34, 571–576.
Fauteux, F., Rémus-Borel, W., Menzies, J.G., Bélanger, R.R., 2005. Silicon and plant disease resistance against pathogenic fungi. FEMS Microbiol. Lett. 249, 1–6.
Fraysse, F., Pokrovsky, O.S., Schott, J., Meunier, J.-D., 2006. Surface properties, solubility and dissolution kinetics of bamboo phytoliths. Geochim. Cosmochim. Acta 70, 1939–1951.
Fraysse, F., Pokrovsky, O.S., Schott, J., Meunier, J.-D., 2009. Surface chemistry and reactivity of plant phytoliths in aqueous solutions. Chem. Geol. 258, 197–206.
Garrels, R.M., Christ, C.L., 1965. Solutions, Minerals, and Equilibria. Harper & Row, New York.
Gérard, F., Mayer, K., Hodson, M., Ranger, J., 2008. Modelling the biogeochemical cycle of silicon in soils: application to a temperate forest ecosystem. Geochim. Cosmochim. Acta 72, 741–758.
Gislason, S.R., Oelkers, E.H., 2003. Mechanism, rates, and consequences of basaltic glass dissolution: II. An experimental study of the dissolution rates of basaltic glass as a function of pH and temperature. Geochim. Cosmochim. Acta 67, 3817–3832.
Gudbrandsson, S., Wolff-Boenisch, D., Gislason, S.R., Oelkers, E.H., 2011. An experimental study of crystalline basalt dissolution from 2⩽ pH⩽ 11 and temperatures from 5 to 75° C. Geochim. Cosmochim. Acta 75, 5496–5509.
Guntzer, F., Keller, C., Poulton, P.R., McGrath, S.P., Meunier, J.-D., 2012. Long-term removal of wheat straw decreases soil amorphous silica at Broadbalk, Rothamsted. Plant Soil 352, 173–184.
Haynes, R.J., 2017. The nature of biogenic Si and its potential role in Si supply in agricultural soils. Agric. Ecosyst. Environ. 245, 100–111.
M. Haysom L. Chapman Some aspects of the calcium silicate trials at 1975 Mackay, Proceedings.
Henriet, C., Bodarwé, L., Dorel, M., Draye, X., Delvaux, B., 2008a. Leaf silicon content in banana (Musa spp.) reveals the weathering stage of volcanic ash soils in Guadeloupe. Plant Soil 313, 71–82.
Henriet, C., De Jaeger, N., Dorel, M., Opfergelt, S., Delvaux, B., 2008b. The reserve of weatherable primary silicates impacts the accumulation of biogenic silicon in volcanic ash soils. Biogeochemistry 90, 209–223.
Henriet, C., Draye, X., Oppitz, I., Swennen, R., Delvaux, B., 2006. Effects, distribution and uptake of silicon in banana (Musa spp.) under controlled conditions. Plant Soil 287, 359–374.
Herbillon, A., 1986. Chemical estimation of weatherable minerals present in the diagnostic horizons of low activity clay soils, Proceedings of the 8th International Clay Classification Workshop: Classification, Characterization and Utilization of Oxisols (part 1)[Beinroth, FH, Camargo, MN and Eswaran (ed.)][39–48](Rio de Janeiro, 1986).
Houben, D., Sonnet, P., Cornelis, J.-T., 2014. Biochar from Miscanthus: a potential silicon fertilizer. Plant Soil 374, 871–882.
Jeffery, S., Verheijen, F.G., Van Der Velde, M., Bastos, A.C., 2011. A quantitative review of the effects of biochar application to soils on crop productivity using meta-analysis. Agric. Ecosyst. Environ. 144, 175–187.
Jones, L., Handreck, K., 1963. Effects of iron and aluminium oxides on silica in solution in soils. Nature 198, 852–853.
Jones, L., Handreck, K., 1965. Studies of silica in the oat plant. Plant Soil 23, 79–96.
Kaczorek, D., Puppe, D., Busse, J., Sommer, M., 2019. Effects of phytolith distribution and characteristics on extractable silicon fractions in soils under different vegetation–An exploratory study on loess. Geoderma 356, 113917.
Keller, C., Guntzer, F., Barboni, D., Labreuche, J., Meunier, J.-D., 2012. Impact of agriculture on the Si biogeochemical cycle: input from phytolith studies. C.R. Geosci. 344, 739–746.
Kelly, E., 1990. Methods for Extracting Opal Phytoliths From Soil And Plant Material. Intern. Rep., Dep. Agron. Colorado State Univ., Fort Collins.
Kittrick, J., 1977. Mineral equilibria and the soil system. Miner. Soil Environ. 1–25.
Klotzbücher, T., Marxen, A., Jahn, R., Vetterlein, D., 2016. Silicon cycle in rice paddy fields: insights provided by relations between silicon forms in topsoils and plant

silicon uptake. Nutr. Cycl. Agroecosyst. 105, 157–168.
Klotzbücher, T., Marxen, A., Vetterlein, D., Schneiker, J., Türke, M., van Sinh, N., Manh, N.H., van Chien, H., Marquez, L., Villareal, S., 2015. Plant-available silicon in paddy soils as a key factor for sustainable rice production in Southeast Asia. Basic Appl. Ecol. 16, 665–673.
Köhler, S.J., Bosbach, D., Oelkers, E.H., 2005. Do clay mineral dissolution rates reach steady state? Geochim. Cosmochim. Acta 69, 1997–2006.
Koning, E., Epping, E., Van Raaphorst, W., 2002. Determining biogenic silica in marine samples by tracking silicate and aluminium concentrations in alkaline leaching solutions. Aquat. Geochem. 8, 37–67.
Lehmann, J., Joseph, S., 2015. Biochar for environmental management: an introduction. In. Biochar for environmental management: Science, Technology and Implementation, Lehmann J. & Joseph S. Eds., Rouledge, London, p. 1-13.
Li, Z., Delvaux, B., 2019. Phytolith-rich biochar: A potential Si fertilizer in desilicated soils. GCB Bioenergy 11, 1264–1282.
Li, Z., Delvaux, B., Yans, J., Dufour, N., Houben, D., Cornelis, J.T., 2018. Phytolith-rich biochar increases cotton biomass and silicon-mineralomass in a highly weathered soil. J. Plant Nutr. Soil Sci. 181, 537–546.
Li, Z., Unzué-Belmonte, D., Cornelis, J.-T., Vander Linden, C., Struyf, E., Ronsse, F., Delvaux, B., 2019. Effects of phytolithic rice-straw biochar, soil buffering capacity and pH on silicon bioavailability. Plant Soil 438, 187–203.
Liang, B., Lehmann, J., Solomon, D., Kinyangi, J., Grossman, J., O'neill, B., Skjemstad, J., Thies, J., Luizao, F., Petersen, J., 2006. Black carbon increases cation exchange capacity in soils. Soil Sci. Soc. Am. J. 70, 1719–1730.
Liang, Y., Sun, W., Zhu, Y.-G., Christie, P., 2007. Mechanisms of silicon-mediated alleviation of abiotic stresses in higher plants: a review. Environ. Pollut. 147, 422–428.
Lindsay, W.L., 1979. Chemical Equilibria in Soils. John Wiley and Sons Ltd.
Liu, X., Li, L., Bian, R., Chen, D., Qu, J., Wanjiru Kibue, G., Pan, G., Zhang, X., Zheng, J., Zheng, J., 2014. Effect of biochar amendment on soil-silicon availability and rice uptake. J. Plant Nutr. Soil Sci. 177, 91–96.
Liu, X., Zhang, A., Ji, C., Joseph, S., Bian, R., Li, L., Pan, G., Paz-Ferreiro, J., 2013. Biochar's effect on crop productivity and the dependence on experimental conditions—a meta-analysis of literature data. Plant Soil 373, 583–594.
Lucas, Y., 2001. The role of plants in controlling rates and products of weathering: importance of biological pumping. Annu. Rev. Earth Planet. Sci. 29, 135–163.
Lucas, Y., Luizao, F., Chauvel, A., Rouiller, J., Nahon, D., 1993. The relation between biological activity of the rain forest and mineral composition of soils. Science 260, 521–523.
Ma, J.F., Takahashi, E., 2002. Soil, Fertilizer, and Plant Silicon Research in Japan. Elsevier.
Major, J., Rondon, M., Molina, D., Riha, S.J., Lehmann, J., 2010. Maize yield and nutrition during 4 years after biochar application to a Colombian savanna oxisol. Plant Soil 333, 117–128.
Marxen, A., Klotzbücher, T., Jahn, R., Kaiser, K., Nguyen, V., Schmidt, A., Schädler, M., Vetterlein, D., 2016. Interaction between silicon cycling and straw decomposition in a silicon deficient rice production system. Plant Soil 398, 153–163.
McKeague, J., Cline, M., 1963a. Silica in soil solutions: I. The form and concentration of dissolved silica in aqueous extracts of some soils. Can. J. Soil Sci. 43, 70–82.
McKeague, J., Cline, M., 1963b. Silica in soil solutions: II. The adsorption of monosilicic acid by soil and by other substances. Can. J. Soil Sci. 43, 83–96.
McKeague, J., Cline, M., 1963c. Silica in soils. In: Advances in Agronomy. Elsevier, pp. 339–396.
Meunier, J., Guntzer, F., Kirman, S., Keller, C., 2008. Terrestrial plant-Si and environmental changes. Mineral. Mag. 72, 263–267.
Meunier, J.D., Colin, F., Alarcon, C., 1999. Biogenic silica storage in soils. Geology 27, 835–838.
Meunier, J.D., Keller, C., Guntzer, F., Riotte, J., Braun, J.J., Anupama, K., 2014. Assessment of the 1% Na2CO3 technique to quantify the phytolith pool. Geoderma 216, 30–35.
Ngoc Nguyen, M., Dultz, S., Guggenberger, G., 2014. Effects of pretreatment and solution chemistry on solubility of rice-straw phytoliths. J. Plant Nutr. Soil Sci. 177, 349–359.
Parfitt, R., 2009. Allophane and imogolite: role in soil biogeochemical processes. Clay Miner. 44, 135–155.
Parfitt, R., Henmi, T., 1982. Comparison of an oxalate-extraction methon and an infrared spectroscopic method for determining allophane in soll clays. Soil Sci. Plant Nutr. 28, 183–190.
Parfitt, R., Russell, M., Orbell, G., 1983. Weathering sequence of soils from volcanic ash involving allophane and halloysite, New Zealand. Geoderma 29, 41–57.
Parfitt, R.L., Furkert, R., Henmi, T., 1980. Identification and structure of two types of allophane from volcanic ash soils and tephra. Clays Clay Minerals 28, 328–334.
Ronsse, F., Van Hecke, S., Dickinson, D., Prins, W., 2013. Production and characterization of slow pyrolysis biochar: influence of feedstock type and pyrolysis conditions. GCB Bioenergy 5, 104–115.
Saccone, L., Conley, D., Koning, E., Sauer, D., Sommer, M., Kaczorek, D., Blecker, S., Kelly, E., 2007. Assessing the extraction and quantification of amorphous silica in soils of forest and grassland ecosystems. Eur. J. Soil Sci. 58, 1446–1459.
Sauer, D., Saccone, L., Conley, D.J., Herrmann, L., Sommer, M., 2006. Review of methodologies for extracting plant-available and amorphous Si from soils and aquatic sediments. Biogeochemistry 80, 89–108.
Savant, N., Snyder, G., Datnoff, L., 1996. Silicon management and sustainable rice production. In: Advances in Agronomy. Elsevier, pp. 151–199.
Smithson, F., 1956. Plant opal in soil. Nature 178, 107.
Sohi, S., Krull, E., Lopez-Capel, E., Bol, R., 2010. A review of biochar and its use and function in soil. Adv. Agron. 105, 47–82.
Sommer, M., Jochheim, H., Höhn, A., Breuer, J., Zagorski, Z., Busse, J., Barkusky, D., Meier, K., Puppe, D., Wanner, M., 2013. Si cycling in a forest biogeosystem–the importance of transient state biogenic Si pools. Biogeosciences 10, 4991–5007.
Sommer, M., Kaczorek, D., Kuzyakov, Y., Breuer, J., 2006. Silicon pools and fluxes in soils and landscapes—a review. J. Plant Nutr. Soil Sci. 169, 310–329.
Song, Z., Wang, H., Strong, P.J., Li, Z., Jiang, P., 2012. Plant impact on the coupled terrestrial biogeochemical cycles of silicon and carbon: implications for biogeochemical carbon sequestration. Earth Sci. Rev. 115, 319–331.
Struyf, E., Smis, A., Van Damme, S., Garnier, J., Govers, G., Van Wesemael, B., Conley, D.J., Batelaan, O., Frot, E., Clymans, W., 2010. Historical land use change has lowered terrestrial silica mobilization. Nat. Commun. 1, 129.
Struyf, E., Smis, A., Van Damme, S., Meire, P., Conley, D.J., 2009. The global biogeochemical silicon cycle. Silicon 1, 207–213.
Unzué-Belmonte, D., Struyf, E., Clymans, W., Tischer, A., Potthast, K., Bremer, M., Meire, P., Schaller, J., 2016. Fire enhances solubility of biogenic silica. Sci. Total Environ. 572, 1289–1296.
Vander Linden, C., Delvaux, B., 2019. The weathering stage of tropical soils affects the soil-plant cycle of silicon, but depending on land use. Geoderma 351, 209–220.
Vandevenne, F., Struyf, E., Clymans, W., Meire, P., 2012. Agricultural silica harvest: have humans created a new loop in the global silica cycle? Front. Ecol. Environ. 10, 243–248.
Vermeire, M.-L., Cornu, S., Fekiacova, Z., Detienne, M., Delvaux, B., Cornélis, J.-T., 2016. Rare earth elements dynamics along pedogenesis in a chronosequence of podzolic soils. Chem. Geol. 446, 163–174.
Wang, M., Wang, J.J., Wang, X., 2018a. Effect of KOH-enhanced biochar on increasing soil plant-available silicon. Geoderma 321, 22–31.
Wang, Y., Xiao, X., Chen, B., 2018b. Biochar impacts on soil silicon dissolution kinetics and their interaction mechanisms. Sci. Rep. 8, 8040.
Xiao, X., Chen, B., Zhu, L., 2014. Transformation, morphology, and dissolution of silicon and carbon in rice straw-derived biochars under different pyrolytic temperatures. Environ. Sci. Technol. 48, 3411–3419.
Yoshida, S., 1981. Fundamentals of rice crop science. Int. Rice Res. Inst.